N. Hosseini and D. W. Matolak, "Wide band channel characterization for low altitude unmanned aerial system communication using software defined radios," 2018 Integrated Communications, Navigation, Surveillance Conference (ICNS), Herndon, VA, 2018, pp. 2C2-1-2C2-9.

WIDE BAND CHANNEL CHARACTERIZATION FOR LOW ALTITUDE UNMANNED AERIAL SYSTEM COMMUNICATION USING SOFTWARE DEFINED RADIOS

Nozhan Hosseini, David W. Matolak
Department of Electrical Engineering
University of South Carolina
Columbia, SC, USA 29208

This paper is accepted to be published in IEEE ICNS conference,Herndon, VA, 2018

Abstract

In the near future, there will be a need for accommodating large populations of fast moving Unmanned Aerial Systems (UAS) operating in uncontrolled, very low level (VLL) (below 500 ft.) airspace. As is well-known, real-time knowledge of the wireless propagation channel is essential for the effective design and optimization of wireless communication systems. In this paper, we propose a software defined radio (SDR) based channel sounder employing a wideband linear frequency modulated continuous wave (FMCW) or chirp waveform technique for low altitude air-to-air (AA) links. This paper discusses both matched filter and heterodyne detector implementations in the receiver, and investigates advantages and disadvantages of both architectures for an SDR implementation in an AA scenario. We also discuss proper windowing techniques in the transmitter to improve sounding resolution. Some proof of concept measurement results using SDRs are presented for a simulated UAS scenario.

I. Introduction

In the near future, very low-level (VLL) aircraft will need to communicate via wideband air-to-air (AA), air-to-ground (AG) and even air-to-satellite (AS) links. These UAS must not interfere with any existing infrastructure or impede efficient air traffic management. Ensuring this requires extremely reliable communications, navigation, and surveillance. NASA's UAS traffic management program [1] is coordinating research and development for VLL conditions, but has not addressed the lower layers of the communications protocol stack, specifically the physical (PHY) and data link layers (DLL), which include a number of key design choices, e.g., waveforms, channels, multiple access, etc. Quantifying radio propagation characteristics is critical for the efficient design of reliable wireless communication systems since the channel can have performance limiting effects.

Growth in the number of aeronautical wireless devices in the national airspace may require operation of some links as second order users. These users would access existing resources when not used by primary users. Many solutions have been proposed in the literature to alleviate spectrum congestion. As an example, for multicarrier schemes such as Orthogonal Frequency Division Multiple Access (OFDMA), the subcarriers can be allocated to users as needed. In order to properly configure such a scheme, one needs to know the channel characteristics, particularly delay spread and Doppler spread. OFDM has been applied for over a decade in terrestrial wireless systems, as it is often an excellent method for high rate bi -directional wireless data communication. It can also be a good candidate for wideband communications to transmit/receive payload data from one Unmanned Aerial System (UAS) to another.

Many studies have been done for estimating channel characteristics, in multiple environments. Such measurements are often termed "sounding." With the growth in use of UAS, aeronautical propagation channels have also been studied in recent years. In many channel measurement campaigns, sophisticated channel sounders were used [2]-[6], but there is limited work on real time sounding in VLL scenarios, particularly with software defined radios (SDRs). Low altitude UAS usually have a limited "maximum payload/takeoff handling weight," therefore using low-weight, low-cost and multi-purpose SDRs as channel sounders can be an attractive solution. Moreover, the flexibility and re-configurability of SDRs can enable easy adjustment of measurement parameters in a short time.

978-1-5386-5679-2/18/$31.00 ©2018 IEEE

Channel sounding is done by exciting the channel with a known input signal. The aim is to estimate some characteristics of the channel. For narrowband channels, this is typically the attenuation, which may include fading. For wideband channels, one desires an estimate of the channel impulse response (CIR), or its Fourier transform, the channel transfer function (CTF). Since most channels have time (and spatial) variation, they are often characterized statistically. For the CIR, one wants the amplitudes, delays, and time variation of all multipath components (MPCs). This enables computation of delay spread and Doppler spreads, which are important to determine the appropriate communication signaling design. Designing a communication system without accurate channel knowledge will yield sub-optimal performance. For example, if a signal's bandwidth is larger than the channel's coherence bandwidth, distortion results, and this must either be mitigated (increasing complexity), or a performance degradation (e.g., larger error probability) must be accepted.

The OFDM multicarrier signal is sensitive to frequency offset and drifts that can be caused by the Doppler effects in rapidly time-varying channels such as VLL AA communication links. Multipath components can also have a detrimental effect on OFDM system performance, where orthogonality of the subcarriers can be lost when the delay spread is significant. Therefore, OFDM systems employ guard intervals to avoid intersymbol interference. During the guard interval, the transmitter can send nothing, or most commonly, a cyclic prefix (CP) which is an exact copy of a segment of the last portion of the OFDM symbol. The length of the guard interval and subcarrier spacing are generally set in advance of transmission [7] [8].

The flexibility and re-configurability of SDRs enables cognitive sounding, which means enabling real time CP length and subcarrier spacing adjustment in order to achieve the best performance in different channel scenarios. Although small commercial SDRs may not be able to perform all sophisticated sounding techniques [9] due to their limitations in bandwidth however, their flexibility and re-configurability are suitable for cognitive sounding in dynamic AA channels.

II. Chirp Channel Sounding Principles

Unmodulated continuous-wave (CW) sounders transmit a single tone with constant frequency. The lack of modulation of the source only allows for determination of Doppler shift and amplitude at that specific frequency. In contrast, a frequency modulated continuous-wave (FMCW) signal, also known as a chirp, employs frequency modulation at the signal source to enable channel transfer function measurements. The FMCW sounder usually transmits a signal that has a linear frequency increase or decrease over a frequency range of B Hz in T seconds, where B/T Hz/s is known as the "sweep rate" and the "time bandwidth product" BT is the "dispersion factor" [9]. Mathematically a chirp signal is expressed as [10]:

$$s(t) = cos\left(\omega_c t + \frac{\mu t^2}{2}\right), -\frac{T}{2} \le t \le \frac{T}{2} \qquad (1)$$

where ω_c is the carrier frequency in radians/s and $\mu = 2\pi(\frac{B}{T})$. As calculated in [9], [10], the spectrum for large time bandwidth values is represented by,

$$S(\omega) = \frac{1}{2}\sqrt{\frac{2\pi}{\mu}} exp\left[-j\left(\frac{\omega^2}{2\mu} + \frac{\pi}{4}\right)\right], -\frac{T}{2} \le t \le \frac{T}{2} \qquad (2)$$

The chirp bandwidth (B) and waveform repetition frequency (WRF) are the main parameters that should be considered in designing chirp signals for sounders. The WRF value is proportional to the reciprocal of the chirp duration, i.e., proportional to $1/T$. The maximum Doppler shift that the chirp sounder can detect depends on the repetition frequency as $WRF \ge 2f_{dmax}$. The channel delay resolution increases as bandwidth increases.

Unlike pulsed-sounders, the spectrum of chirp sounders is predominantly contained within the frequency range of the swept bandwidth, therefore filtering is not necessary prior to transmission (although some filtering is generally applied). Chirp sounder receivers must process the received signal to extract channel characteristics, and there are typically two options for receiver structures. In this paper, we employ both matched filter and heterodyne detectors for our simulations and measurements.

A. Matched Filter Detector

The technique of matched filtering is known to maximize sample time SNR; the matched filter CIR is the (conjugate of the) time-reversed transmit signal pulse. This filtering can also be expressed as a correlation. This correlation enables estimation of the CIR parameters (i.e., MPC delays and amplitudes, and with their time variation Doppler spread can also be estimated. A block diagram of a matched filter detector for a chirp sounder is depicted in Figure 1, where the distorted received signal is convolved with a conjugated time-reversed version of the transmitted chirp signal.

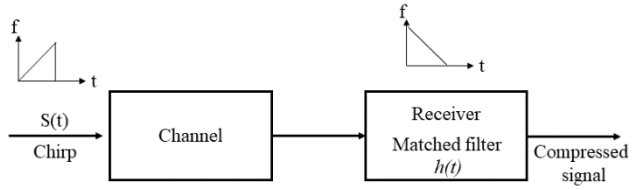

Figure 1. Matched Filter Block Chain

The impulse response of the filter matched to the signal (1) is given by

$$h(t) = kcos\left(\omega_c t - \frac{\mu t^2}{2}\right), -\frac{T}{2} \leq t \leq \frac{T}{2} \qquad (3)$$

where k is an arbitrary real constant. By imposing a unity gain condition at ω_c [10], the matched-filter constant will be

$$k = \sqrt{\frac{2\mu}{\pi}}. \qquad (4)$$

Equation (3) represents a chirp signal with a frequency slope opposite to that of the transmitted signal. The output of the matched filter is found by convolving the chirp signal with the matched filter response, therefore the matched filter accomplishes time compression by delaying the frequencies in their reverse order, thereby bringing all the frequencies back in phase. The output of the matched filter for a chirp signal with a 1 *MHz* bandwidth and one millisecond duration is depicted in Figure 2. The inset shows the result near the peak at 1 ms.

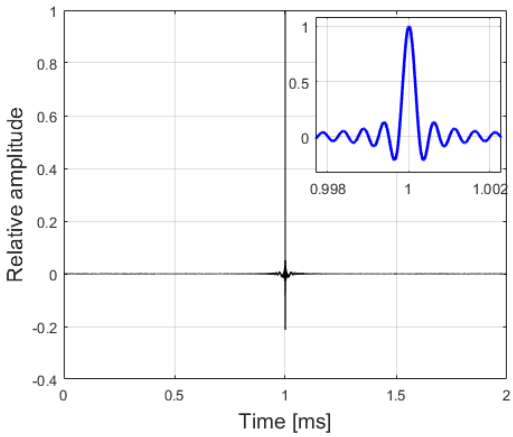

Figure 2. Compressed Signal at Matched Filter Output

As depicted in Figure 2, the envelope of the compressed signal is of the form of a *sin(x)/x* function; is the Fourier transform of a rectangular pulse over the bandwidth of the chirp signal. The success of the matched-filter detector technique in a multipath channel critically depends on producing a compressed-pulse waveform at the output of the matched filter with smaller side-lobes. The amplitude of time domain side-lobes of the compressed signal determine the resolution of multipath components in the sounder. The first and the largest side-lobe is only 13.5 dB below the peak of the compressed pulse and the side-lobes after that decrease by approximately 3 dB per side-lobe interval (Figure 3).

To minimize the effects of these unwanted side-lobes on the system performance, different methods such as windowing have been proposed [10]. In this paper, we weight the transmitted signal in either the time or frequency domain by using various weighting functions. Thus although the theoretical time delay resolution of a chirp signal is *1/B* seconds, practically it also depends on the window function used to reduce the side-lobes of the compressed signal. Proper windowing can increase time delay resolution while it costs in signal-to-noise ratio (SNR). Therefore, there is a tradeoff between resolution and main lobe signal amplitude in designing the window function. Our windowing function is based on an algorithm introduced in [11], and is called Taylor windowing. Although in [9], the Hamming window was mentioned as having the best windowing performance for sounders with noise floor nearly -60 dB relative to desired signal, the main lobe degradation is significant (approximately – 11 dB). A

comparison these different windowing functions is depicted in Figure 3.

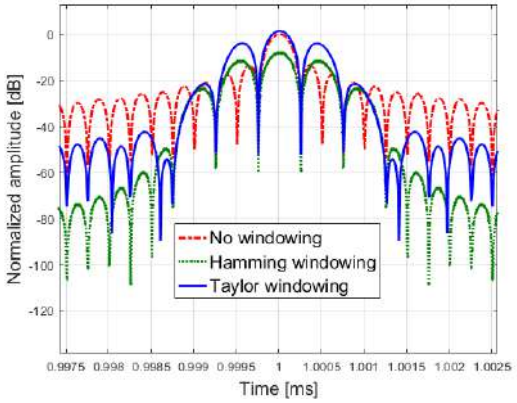

Figure 3. Comparison between Two Well-Known Windowing Functions

In Figure 3 the amplitude of the Hamming main lobe is smaller than for the other two, but its side lobes are lower. Taylor windowing on the other hand has a tradeoff between Hamming and no windowing.

B. Heterodyne Detector

The technique of heterodyne detection is based on multiplication of the received signal by a delayed replica of the transmitted signal $y(t-\tau_0)$. The frequency sweeps upward linearly, then the output of the multiplication is low pass filtered. The spectrum of the receiver output is then analyzed to achieve the *sin(x)/x* compression. The block diagram is depicted in Figure 4.

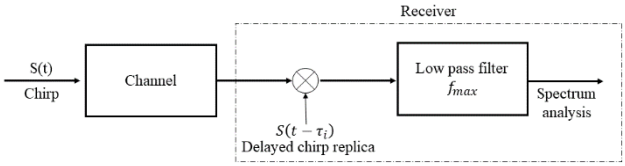

Figure 4. Heterodyne Detector Block Diagram

Assuming an ideal channel, the output of the heterodyne mixer can be represented mathematically as

$$A_i s(t-\tau_i)s(t) = A_i cos\left(\omega_c t + \frac{\mu t^2}{2}\right) \times cos\left[\omega_c(t-\tau_i) + \frac{\mu(t-\tau_i)^2}{2}\right] \quad (5)$$
$$= \frac{A_i}{2}\cos\left[2\omega_c t - \omega_c\tau_i + \frac{\mu}{2}t^2 + \frac{\mu}{2}(t-\tau_i)^2\right] + \frac{A_i}{2}\cos\left[\omega_c\tau_i + \frac{\mu}{2}t^2 - \frac{\mu}{2}(t-\tau_i)^2\right].$$

After applying a low-pass filter the first term is removed, therefore the frequency of the remaining term is given by

$$f_i = \frac{d\left[\omega_c\tau_i + \frac{\mu}{2}t^2 - \frac{\mu}{2}t^2 - \frac{\mu}{2}\tau_i^2 + \mu t\tau_i\right]}{2\pi dt} = \frac{\mu\tau_i}{2\pi} = \frac{B}{T}\tau_i, \quad (6)$$

where τ_i is the time difference between the original chirp signal and the locally generated signal. Thus, the filter cutoff-frequency $f_{\max}$ should be chosen in a way to accommodate the time delay τ_{max} of the longest-delay MPC with frequency of $\left(\frac{B}{T}\right)\tau_{max}$.

The advantage of a heterodyne detector compared to the matched filter detector is that the heterodyne detector compresses the signal in frequency instead of time, and this feature enables the use of low bandwidth digitizers and channel data acquisition, where digitizer bandwidth depends on the maximum time delay or the range of the farthest multipath component. This behavior is favorable for current SDRs that are limited in data acquisition speed. However, matched filter detection gives the multipath structure in real time as the output consists of the time-compressed signal, whereas the heterodyne detector requires a post processing spectrum analyzer to perform the same function. Therefore, applying fast Fourier transform (FFT) over a single sweep gives a *sin(x)/x* main lobe centered at the frequency corresponding to the time delay between transmitter chirp and replica in the receiver.

In the post-processing step, applying the FFT algorithm gives a spectrum that is extended in frequency from zero to half the sampling frequency f_s, thus these samples can be scaled to the time delay domain using sweep rate *B/T* according to $\tau_i = \left(\frac{T}{B}\right) f_i$, where τ_i is the time delay of the *i*th multipath component.

III. Channel Modeling and Simulations

Our proposed scenario is characterization of a moderately dense environment with several multipath components for AA communication between two VLL UASs moving in random directions with relative speed of Δv as depicted in Figure 5 (a). An example impulse response of the channel is also plotted in Figure 5 (b), based on the objects present in Figure 5 (a). Note that the number of multipath components could be different in general.

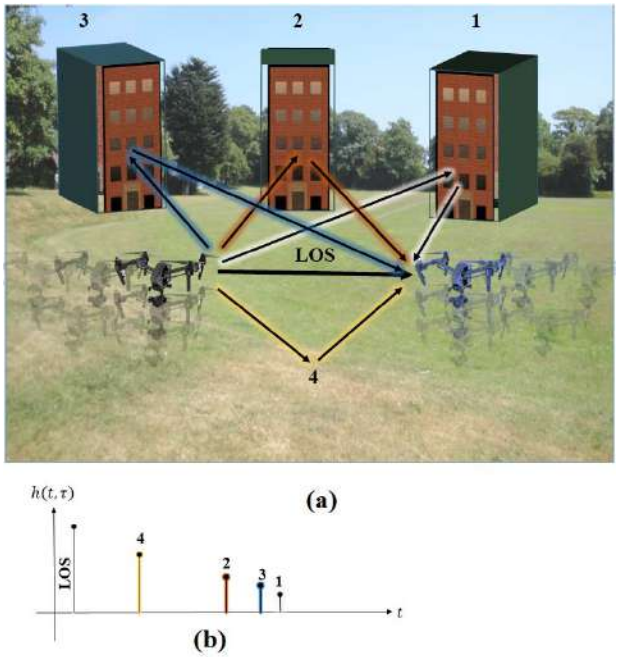

Figure 5. Example Channel Environment with Example Impulse Response

In this scenario, assuming two UAS with relative speed of Δv maneuvering and communicating at frequency f_0 and based on (7) yields a Doppler bandwidth of Δf. Therefore in our channel sounding we require a chirp with WRF value larger than $(2f_{dmax})$ where f_{dmax} is the maximum detectable Doppler frequency shift.

$$\Delta f = \frac{\Delta v f_0}{c} cos\theta \qquad (7)$$

In (7) c is the speed of electromagnetic wave in the air, and θ is the angle between propagation and relative velocity vectors. As an example, for $f_0 = 2.42$ GHz and Δv =30 miles/hr (13.4 m/s) the maximum Doppler shift is $\Delta f \cong 108.1$ Hz. Thus, based on previous criteria, the chirp signal WRF should be at least 216.1 Hz. However, to allow a margin for additional shifts due to receiver oscillator frequency offsets, our Doppler shift range is set to 250 Hz. Considering a chirp signal with bandwidth $B = 25$ MHz, the minimum nominal time delay resolution will be 40 ns, which corresponds to a 12 m minimum distance difference between line-of-sight (LOS) and multipath components in order to be resolvable in our channel sounder power delay profile (PDP). Considering all the criteria described in the example channel scenario, we generated a chirp FMCW waveform with parameters defined in Table 1.

Table 1. Proposed FMCW Waveform Parameters

Parameter	Value
Center frequency	2.42 GHz
Bandwidth (B)	25 MHz
WRF (1/T)	500 Hz
Sampling rate	50 MHz

AA communication between two moving VLL entities can be described as via a strong LOS path signal and signals that arrive at the receiver by several different paths due to reflections from obstacles in the environment. This channel can be simulated as a frequency selective fading Ricean stochastic model in a pre-defined radio channel propagation scenario described in Table 2.

Table 2. Proposed Channel Parameters

Parameter	Value
Number of MPCs	4
PDP delay vector	[0, 30, 140, 290, 330] ns
Normalized MPC magnitudes	[1, 0.4, 0.1, 0.07, 0.04]
Total relative speed Δv	30 miles/hr
Channel fading model	Ricean, *K*=8 dB
Noise floor amplitude	-100 dB
Maximum Doppler frequency	108.1 Hz

Our simulated channel model is adapted from [12], where an improved sum-of-sinusoids (SOS) based model was proposed for the accurate simulation of time-correlated and frequency selective Ricean fading channels. Filter-based models are usually based on passing a Gaussian process through a linear filter with a transfer function equal to the square root of the Doppler power spectral density (PSD), but this method can have higher computational complexity [13]. Both models are well established. We add additive white Gaussian noise (AWGN) with noise floor relative amplitude of -100 dB.

For matched filter simulations, we generated the chirp signal according to Table 1 parameters. We weighted the signal by a Taylor window function, then input it to the SOS based frequency selective fading model. Then the output of the channel simulator was convolved with a time-reversed version of the transmitted chirp signal, as described in subsection II.A. In Figure 6 (a) we show a time compressed version view of all PDPs. The MPC delay values are more distinguishable in the "top view" of Figure 6 (b). As described in Table 2, four multipath components were present, at delays of 30, 140, 290 and 330 ns. The first component with delay of 40 ns was not resolvable, and hence was combined with the LOS component.

To obtain the delay Doppler spectrum and time variability of the simulated channel, analysis over a number of sweep times is performed, which is possible by taking the Fourier transform over *N* sweeps, where the spectrum is also in the form of a *sinc* function with frequencies centered at the Doppler shift frequencies. The corresponding delay Doppler spectrum is depicted in Figure 6 (c).

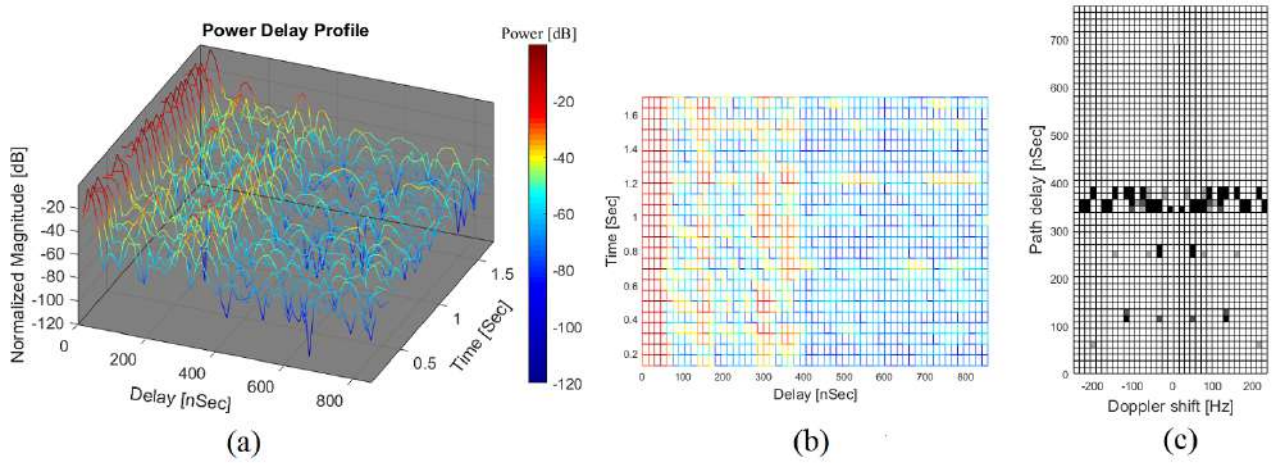

Figure 6. Matched Filter Results: (a) PDP, (b) PDP Top View, and (c) Delay Doppler Spectrum

For heterodyne simulations, spectrum analysis applied to the output of the detector was employed, with the low pass filter cut off frequency set to 2.5 kHz, corresponding to 400 ns as described in Section II.B. As expected, results from the heterodyne detector in Figure 7 show more distinguishable multipath components, due to the structure of the heterodyne detector, while the Doppler spectrum conveys essentially the same information as from the matched filter detector.

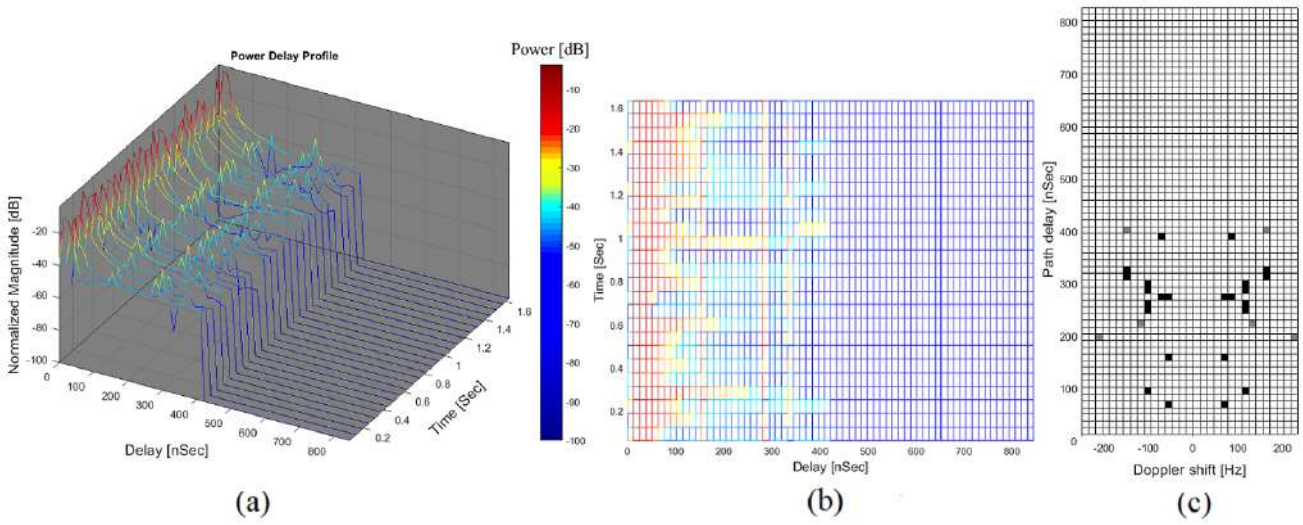

Figure 7. Heterodyne Detector Results: (a) PDP, (b) PDP Top View, and (c) Delay Doppler Spectrum

IV. Measurement Results

For proof of design and concept, we conducted a simple outdoor measurement. The chirp measurement setup parameters are based on those listed in Table 1. A block diagram for the sounding measurement is presented in Figure 8. The selected SDR model for this measurement was the Ettus N210 with the UBX40 daughterboard and a 5 dB gain omni-directional antenna.

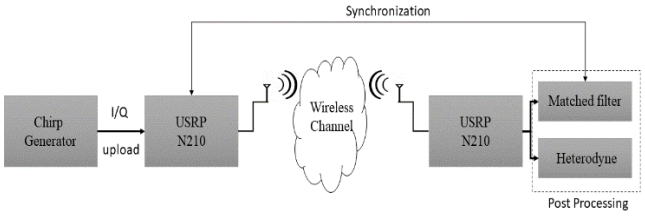

Figure 8. Block Diagram of SDR Sounder Experiment

The complex chirp signal samples were generated in MATLAB® and fed as I/Q complex data to the transmitter that up-converts the signal to the 2.43 GHz radio frequency. At the receiver, the distorted signal is captured by the second USRP. Then the data is input to the SDR heterodyne detector designed in GNURadio (an open source toolkit software for SDRs). The matched filter detector requires synchronization for precise sweep length match, therefore in our measurements we employed the heterodyne detector.

As illustrated in Figure 9, our transmitter was mounted on top of the University of South Carolina Swearingen Engineering Building to emulate a low altitude UAS hovering situation. This transmitter sent its signal with a downtilted omni-directional antenna so that its main lobe was projected on the street with the receiver. The other SDR, as receiver, was mounted on top of a 2007 Mazda 6 car roof.

Figure 9. Measurement Environment

The car speed increased to approximately 30 miles per hour and stayed constant over the path depicted with the red line in Figure 9, and then reduced its speed stop at the end of the street (lower left).

Note that in our USRP the total number of samples to be stored using the heterodyne detector is $2B\tau_{max}$ where τ_{max} is the maximum expected time

delay. This value is significantly lower than the $2BT$ of the matched filter. An example measured PDP from a single sweep is depicted in Figure 10 where a significant LOS component arrived along with other smaller magnitude multipath components. Figure 11 (a) (b) shows measured PDPs during the measurement. As we expected, most of the dominant multipath components had delays close to that of the main LOS component (and were hence unresolvable), however due to the movement of the RX we expect Doppler shifts and possible receiver oscillator frequency offset. Figure 11 (c) presents the measured delay Doppler spectrum result for this test. The maximum value of just over 100 Hz is clear, along with a range of smaller values corresponding to the $\cos\theta$ term scaling of (7).

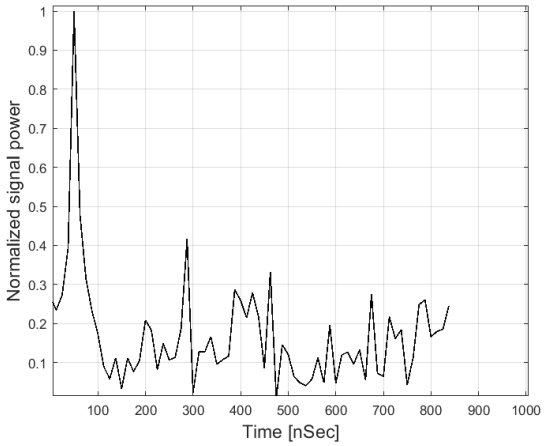

Figure 10. Single Measured PDP

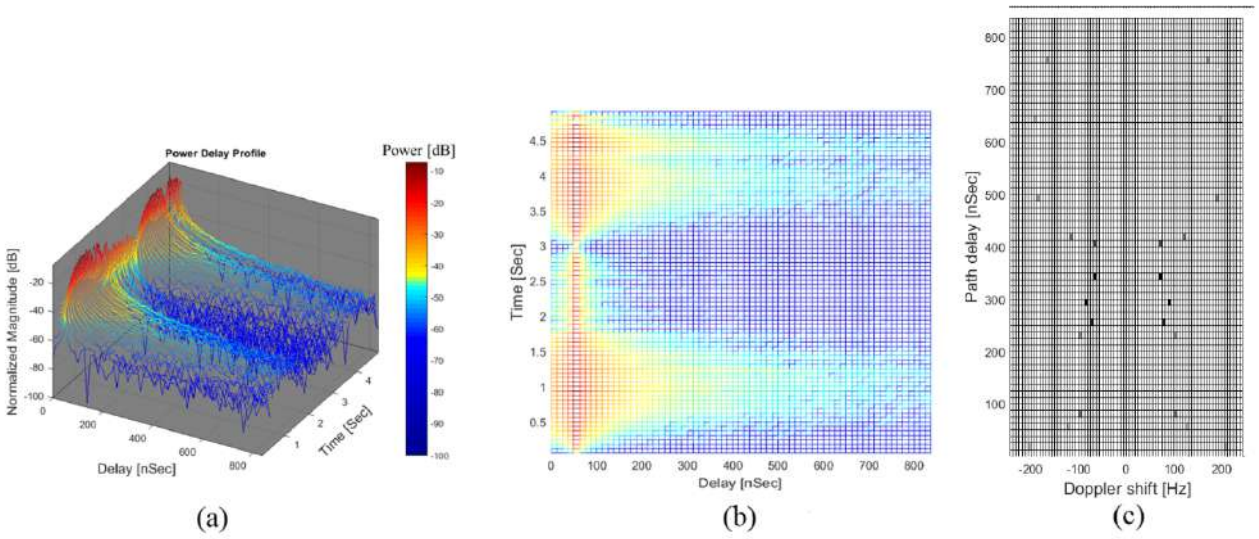

Figure 11. Measurement Results Showing (a) PDPs Over Time, (b) PDPs in "Contour" View, and (c) Delays vs. Doppler Shifts

V. Conclusion

We discussed an implementation of FMCW (chirp) sounders using SDRs for VLL UAS. A motivation for using commercial SDRs was described, along with proper choice of waveform and parameters. We reviewed two types of chirp detectors and discussed their relative merits. Experimental results were provided for an emulated UAS experiment, illustrating the ability of the SDR chirp sounder to yield estimates of channel power delay profiles and scattering functions (delay-Doppler functions). In the near future, state of the art technology plus proper design of algorithms can make SDRs very high-resolution sounders. For future work, we plan to use SDRs mounted on moving objects such as small VLL UAS to gather additional data and refine our processing techniques for channel measurements and modeling.

References

[1] "Unmanned Aircraft System (UAS) Traffic Management (UTM)," https://utm.arc.nasa.gov, Oct. 20, 2017 [Dec. 29, 2017]

N. Hosseini and D. W. Matolak, "Wide band channel characterization for low altitude unmanned aerial system communication using software defined radios," 2018 Integrated Communications, Navigation, Surveillance Conference (ICNS), Herndon, VA, 2018, pp. 2C2-1-2C2-9.

[2] D. W. Matolak, I. Sen, and W. Xiong, “The 5-GHz Airport Surface Area Channel - Part I: Measurement and Modeling Results for Large Airports,” IEEE Trans. Veh. Technol., vol. 57, no. 4, pp. 2014–2026, 2008.

[3] I. Sen and D. W. Matolak, “The 5-GHz Airport Surface Area Channel- Part II: Measurement and Modeling Results for Small Airports,” IEEE Trans. Veh. Technol., vol. 57, no. 4, pp. 2027–2035, 2008.

[4] S. Gligorevic, R. Zierhut, T. Jost, and W. Wang, “Airport Channel Measurements at 5.2 GHz,”Proc. 3rd European Conf. Antennas and Propagation (EuCAP), Berlin, 23-27 March 2009.

[5] S. Gligorevic, T. Jost and M. Walter,” Scatterer Based Airport Surface Channel Model,” IEEE/AIAA 28th Digital Avionics Systems Conf., Orlando, FL, 25-29 October 2009.

[6] C. Bluemm, C. Heller, B. Fourestie and R. Weigel,” Air-to-Ground Channel Characterization for OFDM Communication in C-Band,” 7th Int. Conf. Signal Processing and Communication Systems (ICSPCS), Gold Coast, Australia, 16-18 December 2013.

[7] P. Y. Tsai, T. D. Chiueh, OFDM Baseband Receiver Design for Wireless Communications, Wiley, Singapore, 2007.

[8] A. Ramadan Ali, T. J.Khanzada and A. Omar, ”Adaptive Guard Interval Length for OFDM-Based WLAN Systems in Frequency Selective Channels,” European Conference on Wireless Technology, Amsterdam, Netherlands, 27-28 October 2008.

[9] A. G. Siamarou and M. Al-Nuaimi, "A Wideband Frequency-Domain Channel-Sounding System and Delay-Spread Measurements at the License-Free 57- to 64-GHz Band," IEEE Trans. Instrumentation and Measurement, vol. 59, no. 3, pp. 519-526, March 2010.

[10] S. Salous, Radio Propagation Measurement and Channel Modeling, John Wiley & Sons, Chichester, UK, 2013.

[11] C. Cook, Radar Signals: an Introduction to Theory and Application, Elsevier, 2012

[12] C. G. Walter, R. M. Majewski, and R. S. Goodman, Spotlight Synthetic Aperture Radar: Signal Processing Algorithms,Appendix D.2, Artech House, Boston, MA, 1995.

[13] A. Alimohammad, S. F. Fard, B. F. Cockburn and C. Schlegel, “Compact Rayleigh and Rician Fading Simulator Based on Random Walk Processes,” IET Communications, vol. 3, no. 8, pp. 1333-1342, August 2009.

[14] M. A. Wickert and J. Papenfuss, ”Implementation of a Real-Time Frequency-Selective RF Channel Simulator Using a Hybrid DSP-FPGA Architecture,” IEEE Trans. Microwave Theory and Techniques, vol. 49, no. 8, pp. 1390-1397, Aug 2001.